

Electronic Supplementary Information

Amine-fleshed gold nanoparticles encapsulated in silica nanospheres highly active for catalytic decomposition of formic acid

Mahendra Yadav,^a Tomoki Akita,^a Nobuko Tsumori,^{a,b} and Qiang Xu^{a*}

^a National Institute of Advanced Industrial Science and Technology (AIST), Ikeda, Osaka 563-8577, Japan

Fax: +81 72 751 9629; Tel: +81 72 751 9562 ; E-mail : q.xu@aist.go.jp

^b Toyama National College of Technology, 13, Hongo-machi, Toyama, 939-8630, Japan

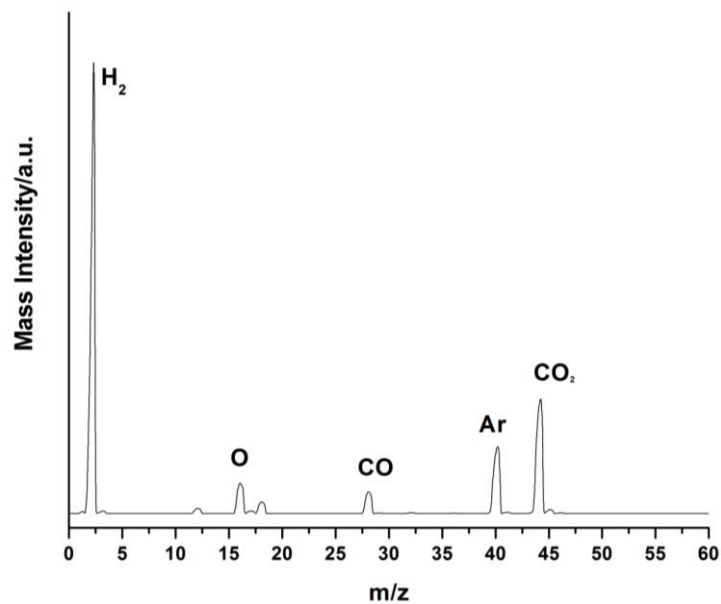


Fig. S1. Mass spectral profile for physical mixture of H₂ and CO₂ (1:1) as a reference gas sample.

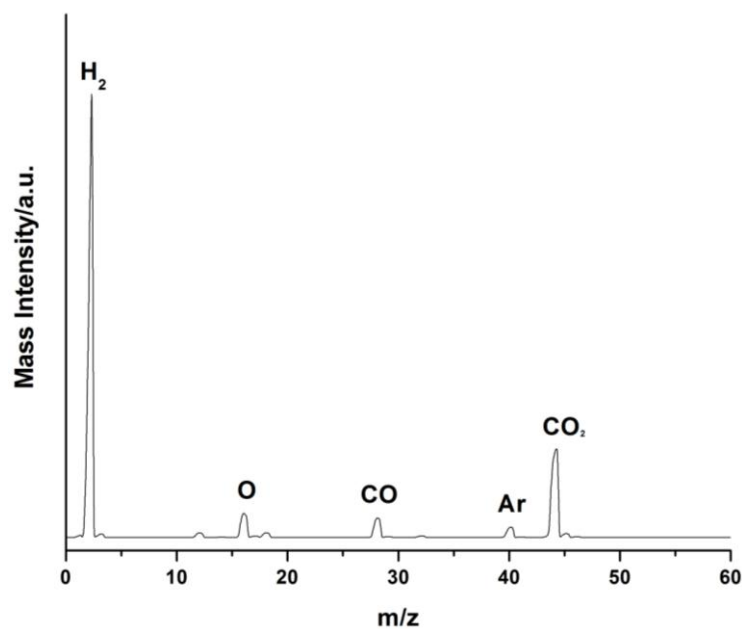


Fig. S2. Mass spectral profile of the released gas from the aqueous solution (1.0 mL) of formic acid (3.0 M) and sodium formate (1.0 M) in the presence of Au@SiO₂-AP catalyst (60 mg) at 90°C.

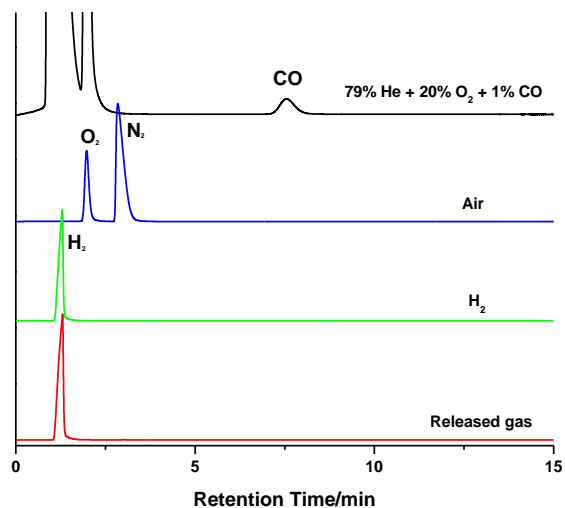


Fig. S3. Gas chromatograms of H₂, air and CO as reference gases and the released gas from the aqueous solution (1.0 mL) of formic acid (3.0 M) and sodium formate (1.0 M) in the presence of Au@SiO₂_AP catalyst (60 mg) at 90°C, showing the presence of H₂ and absence of CO in the generated gas.

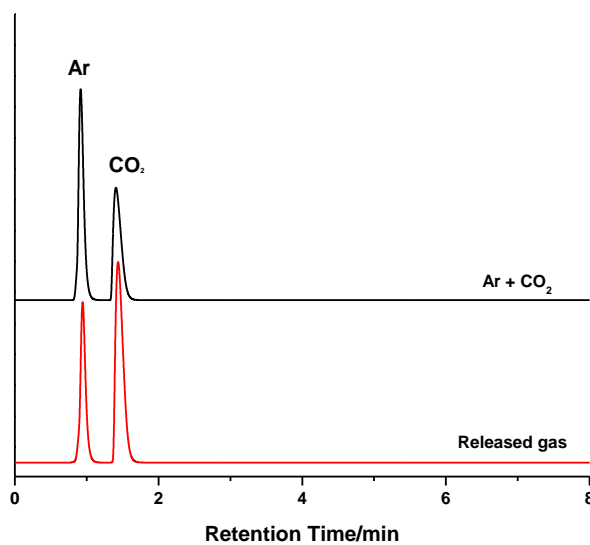


Fig. S4. Gas chromatograms of generated gas from the aqueous solution (1.0 mL) of formic acid (3.0 M) and sodium formate (1.0 M) in the presence of Au@SiO₂_AP catalyst (60 mg) at 90°C, showing the presence of CO₂ in the generated gas.

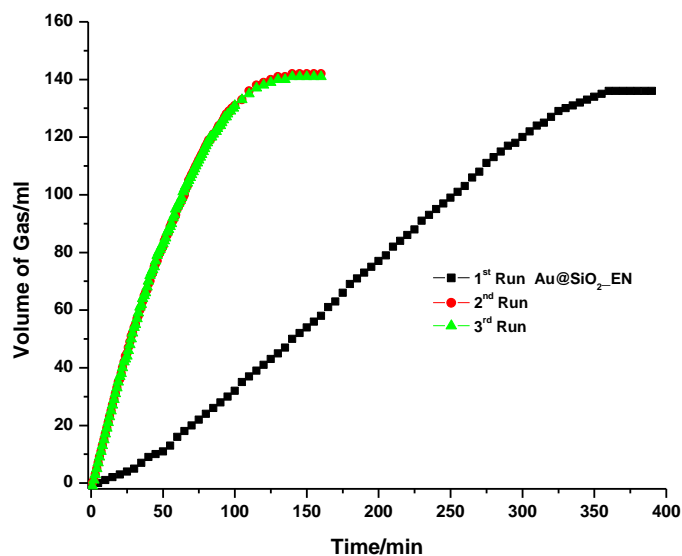


Fig. S5. Time-course plots for hydrogen generation from the aqueous solution (1.0 mL) of formic acid (3.0 M) and sodium formate (1.0 M) in the presence of Au@SiO₂_EN catalyst (60 mg) at 90°C.

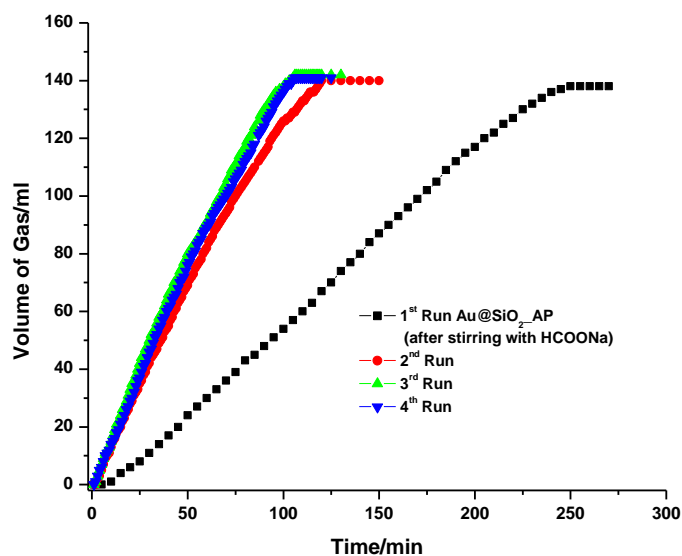


Fig. S6. Time-course plots for hydrogen generation from the aqueous solution of formic acid (3.0 M) in the presence of Au@SiO₂_AP (60 mg) after stirring with the aqueous solution (1.0 mL) of sodium formate (1.0 M) for 240 min at 90°C.

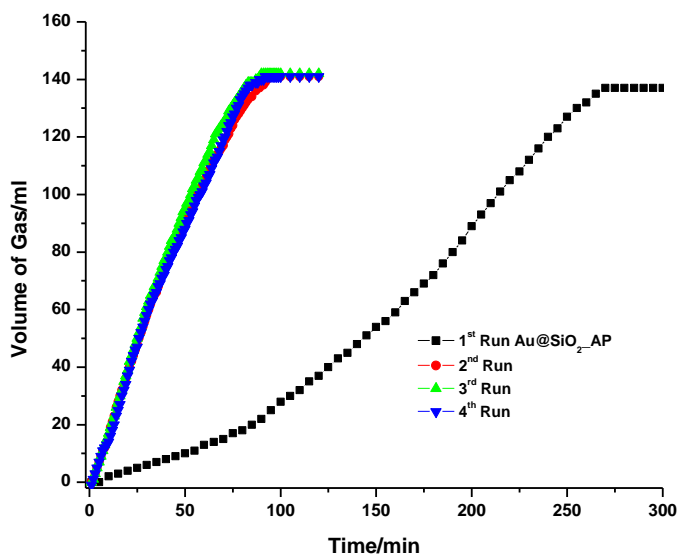


Fig. S7. Time-course plots for hydrogen generation from the aqueous solution (1.0 mL) of formic acid (3.0 M) in the presence of Au@SiO₂-AP catalyst (60 mg) at 90°C.

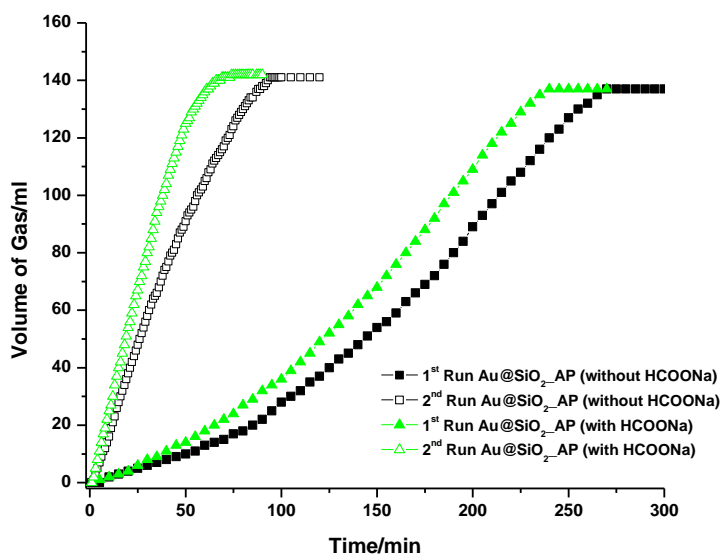


Fig. S8. Time-course plots for hydrogen generation from the aqueous solution (1.0 mL) of formic acid (3.0 M) in the presence of Au@SiO₂-AP (60 mg) with and without sodium formate (1.0 M).

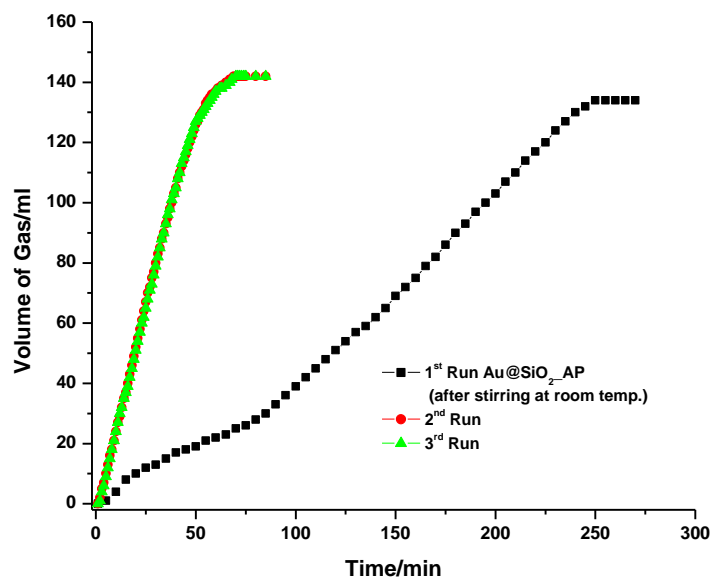


Fig. S9. Time-course plots for hydrogen generation from the aqueous solution (1.0 mL) of formic acid (3.0 M) and sodium formate (1.0 M) in the presence of Au@SiO₂-AP catalyst (60 mg) after stirring for 240 min at room temperature.

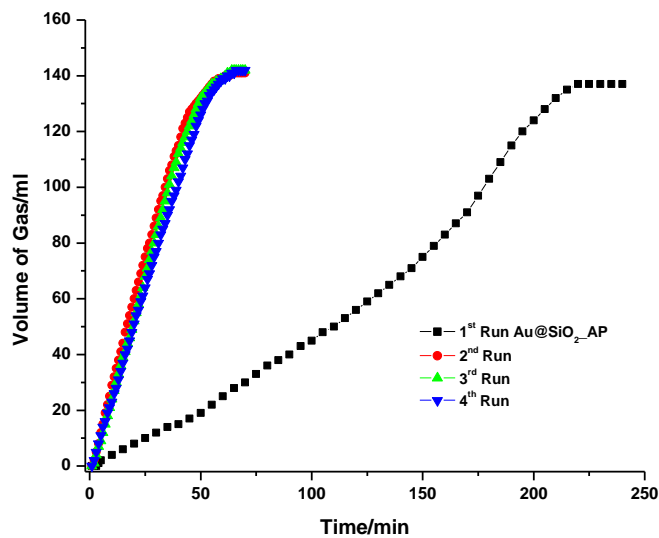


Fig. S10. Time-course plots for hydrogen generation from the aqueous solution (1.0 mL) of formic acid (3.0 M) and sodium formate (1.0 M) in the presence of Au@SiO₂-AP catalyst (prepared by using hydrazine as the reducing agent) (60 mg).

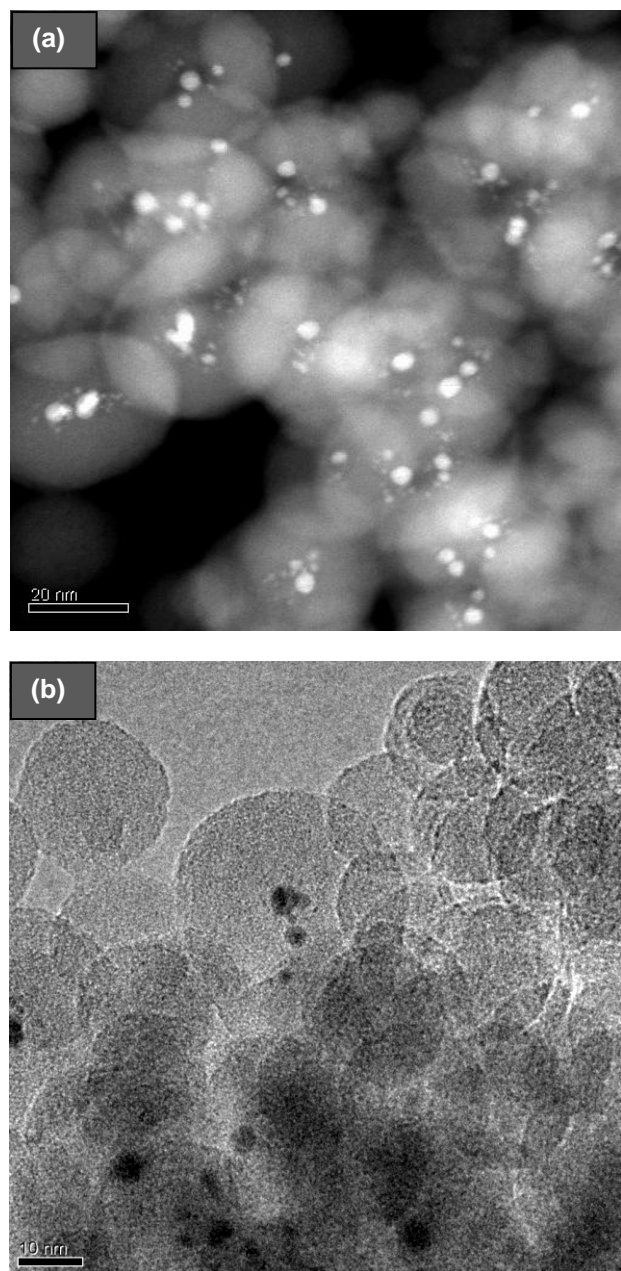


Fig. S11. Representative HAADF-STEM image (a) and TEM image (b) of Au@SiO₂ before catalytic reaction.

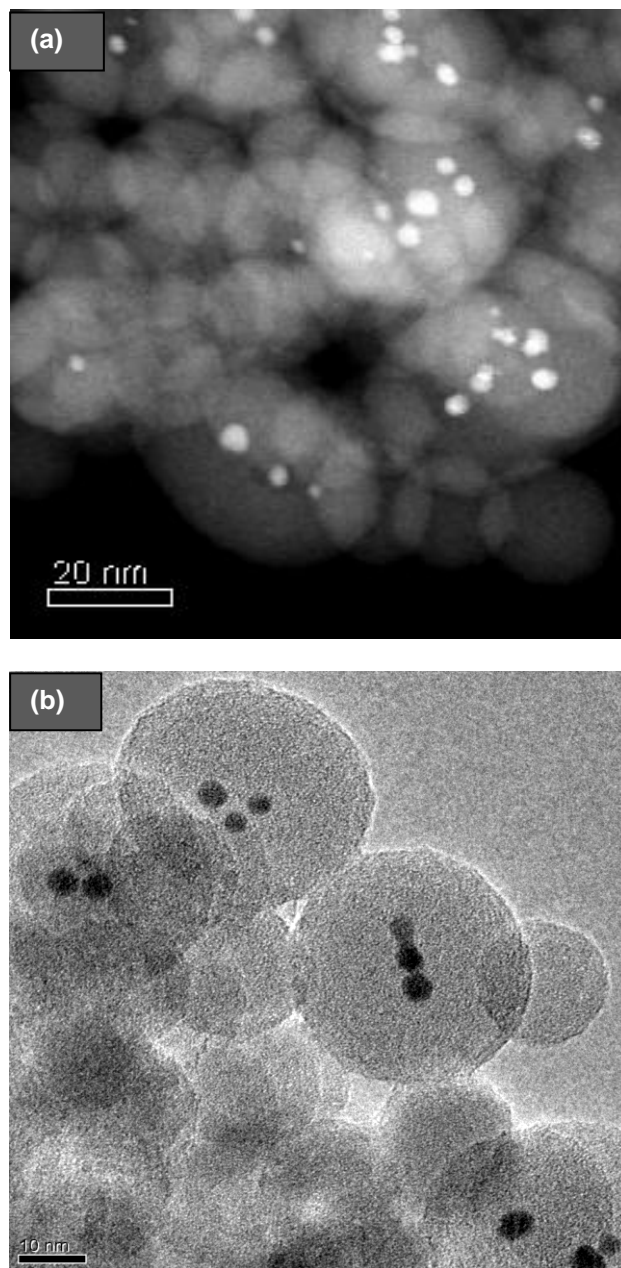


Fig. S12. Representative HAADF-STEM image (a) and TEM image (b) of Au@SiO₂ after catalytic reaction.

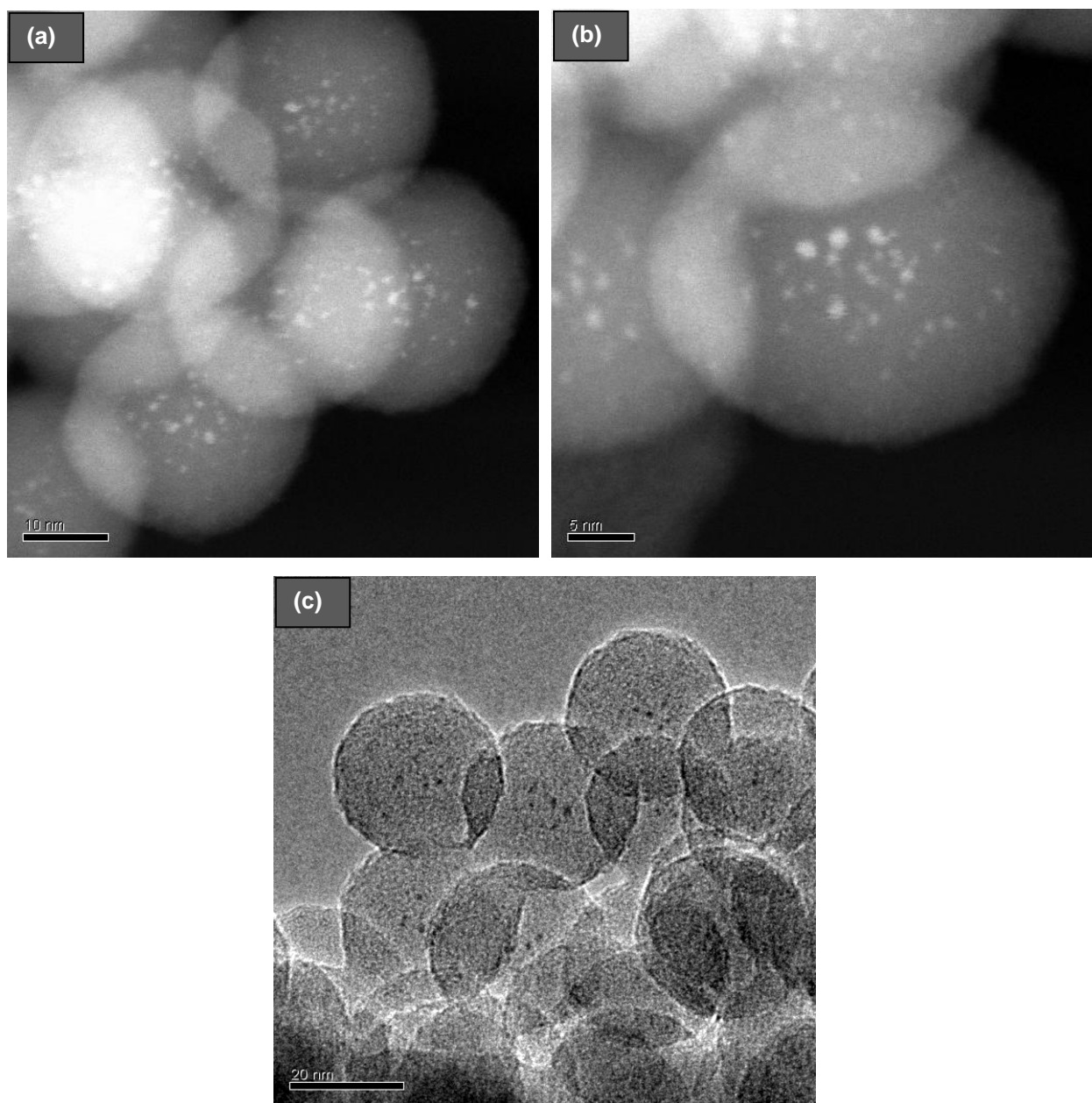


Fig. S13. Representative HAADF-STEM images (a,b) and TEM image (c) of Au@SiO₂_EN before catalytic reaction.

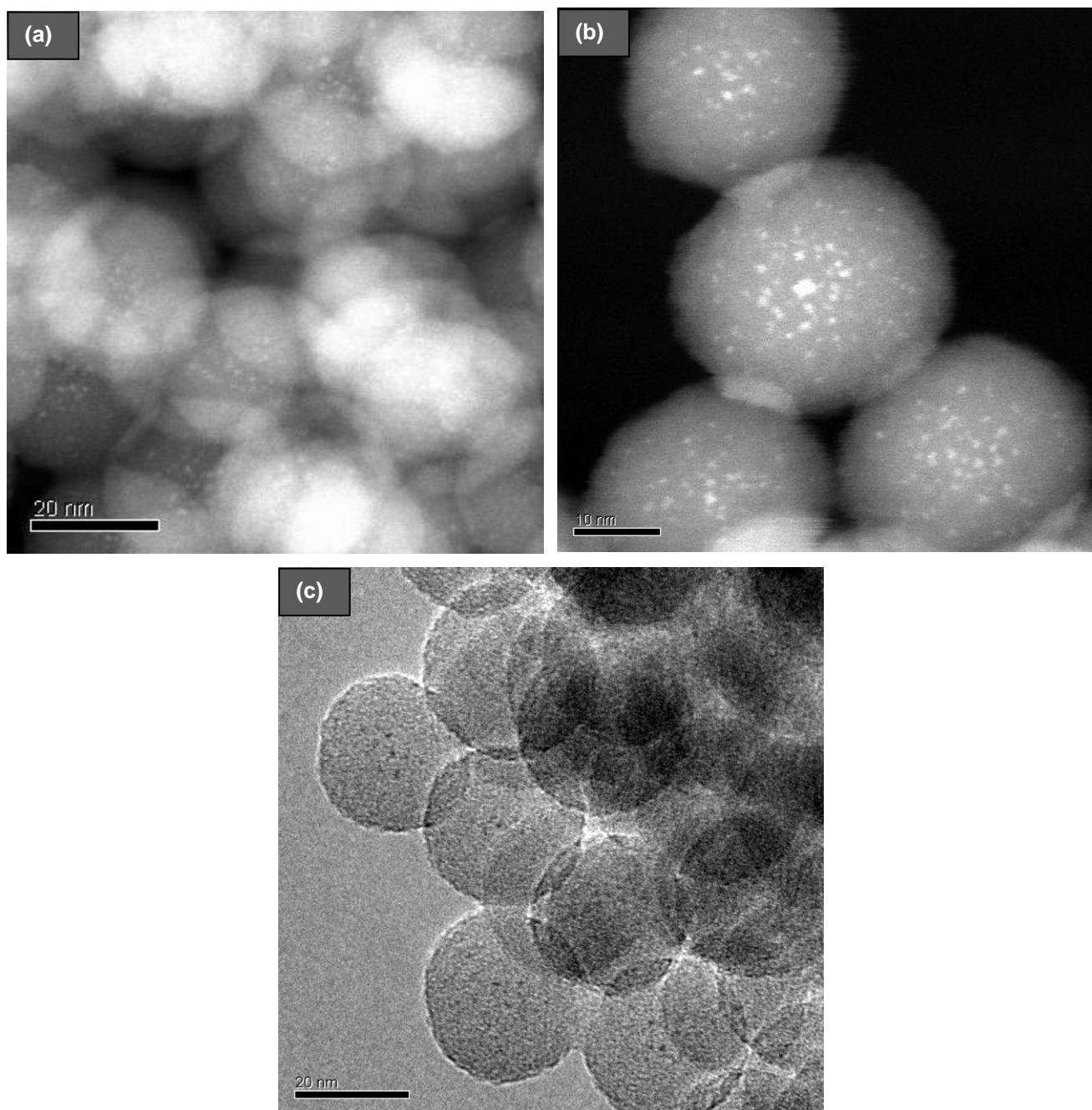


Fig. S14. Representative HAADF-STEM images (a,b) and TEM image (c) of Au@SiO₂_EN after catalytic reaction.

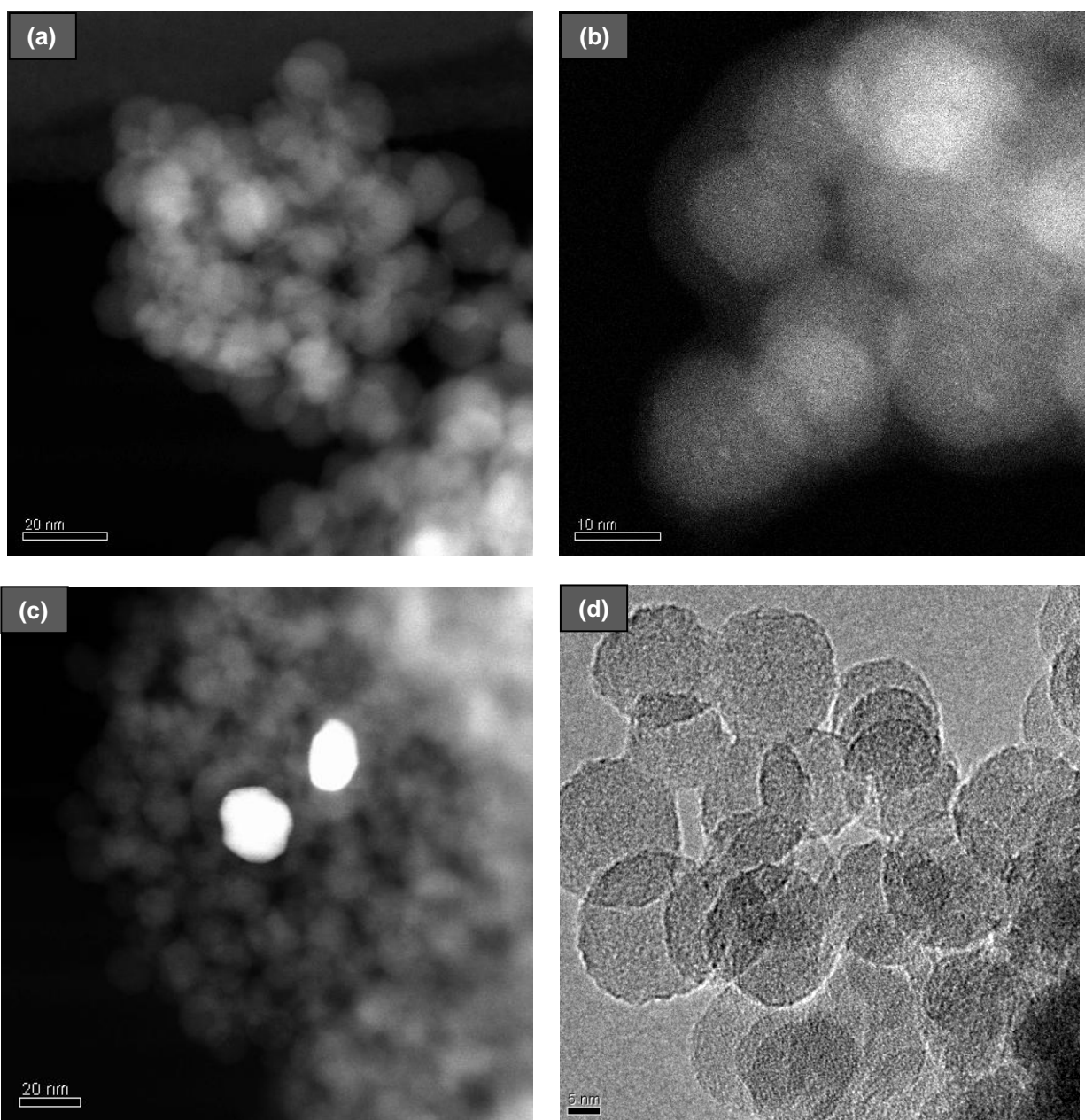


Fig. S15. Representative HAADF-STEM images (a-c) and TEM image (d) of Au@SiO₂-AP before catalytic reaction.

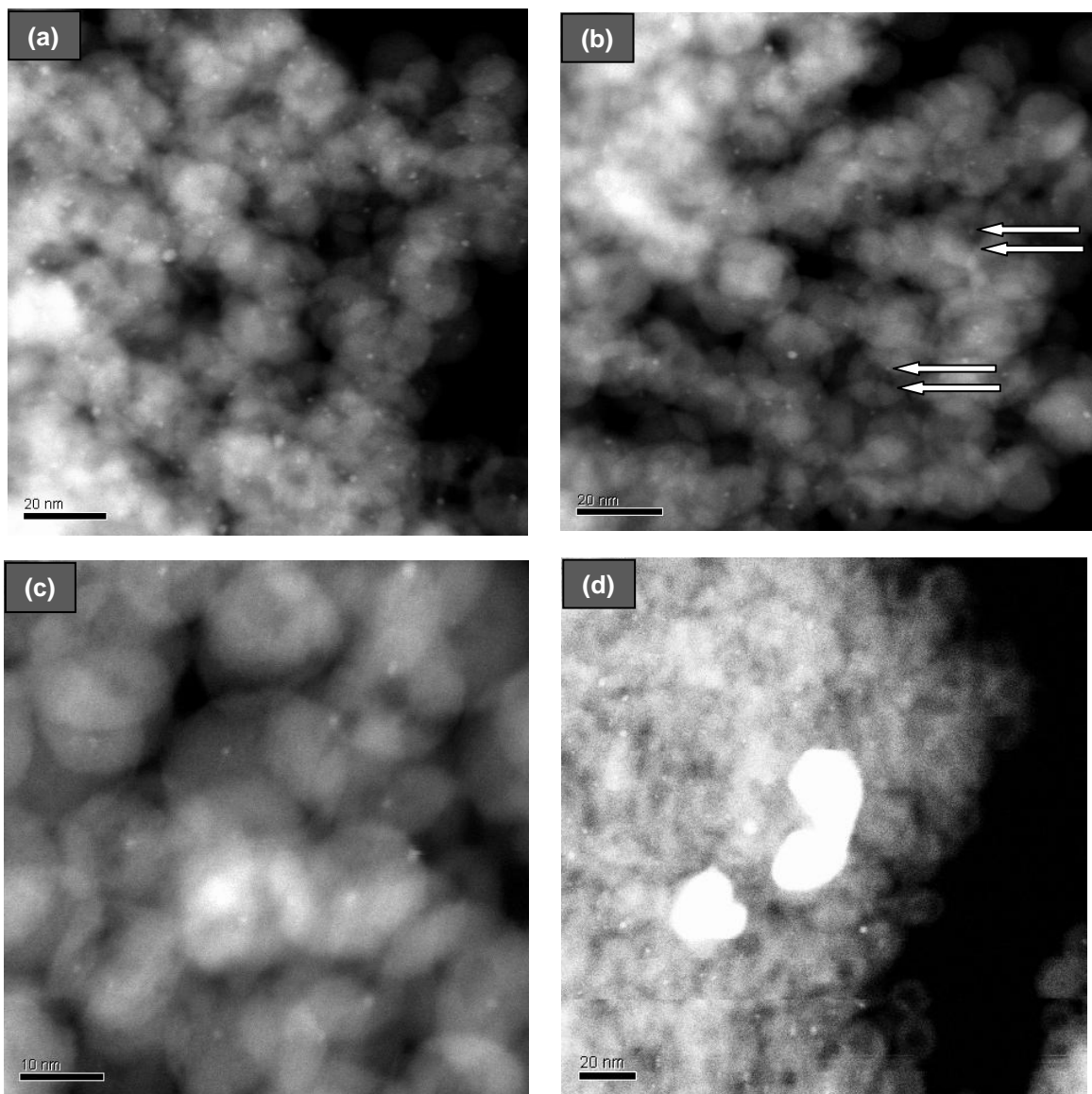


Fig. S16. Representative HAADF-STEM images (a-d) of Au@SiO₂-AP after catalytic reaction.

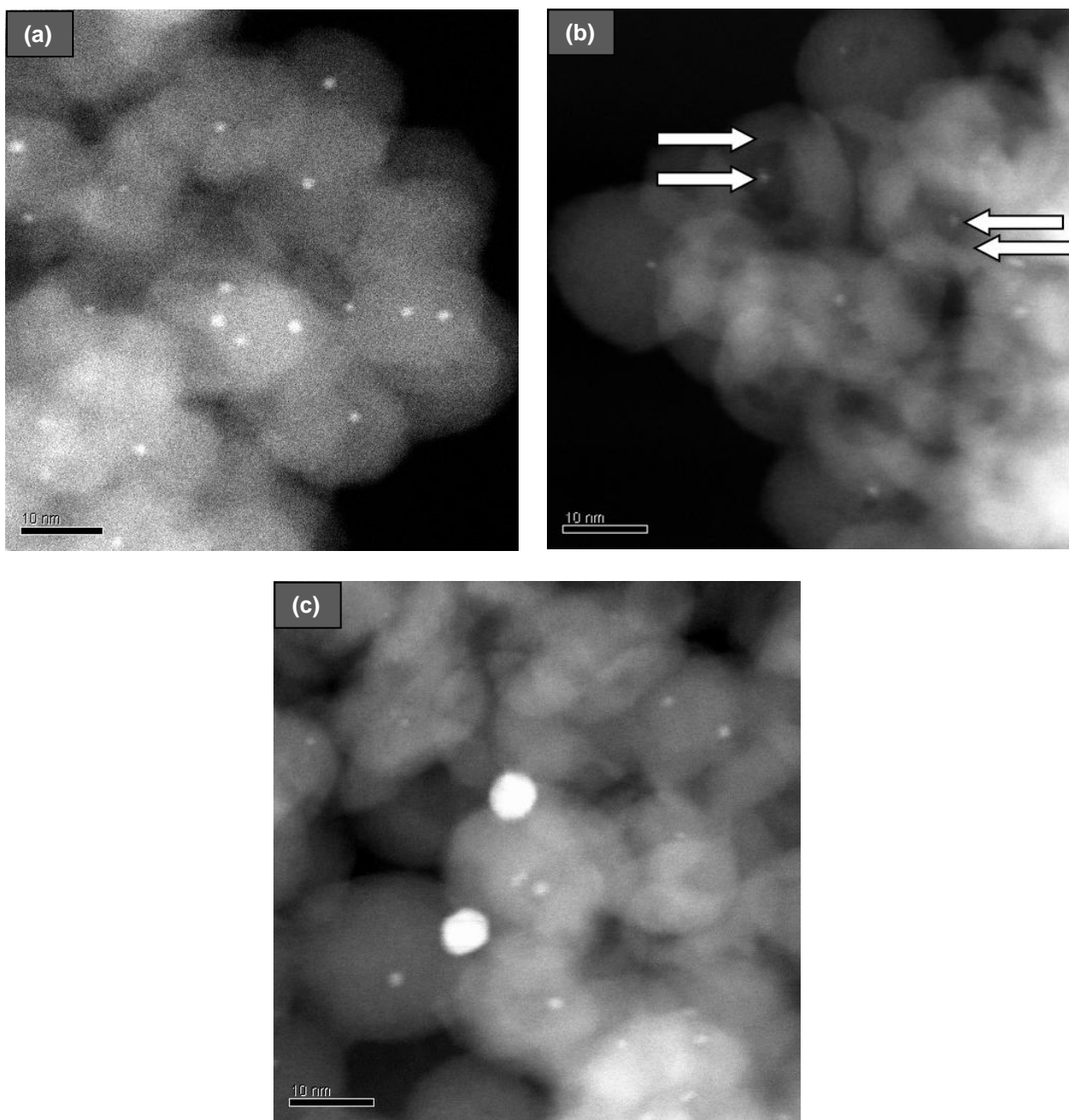


Fig. S17. Representative HAADF-STEM images (a-c) of Au@SiO₂-AP-C before catalytic reaction.

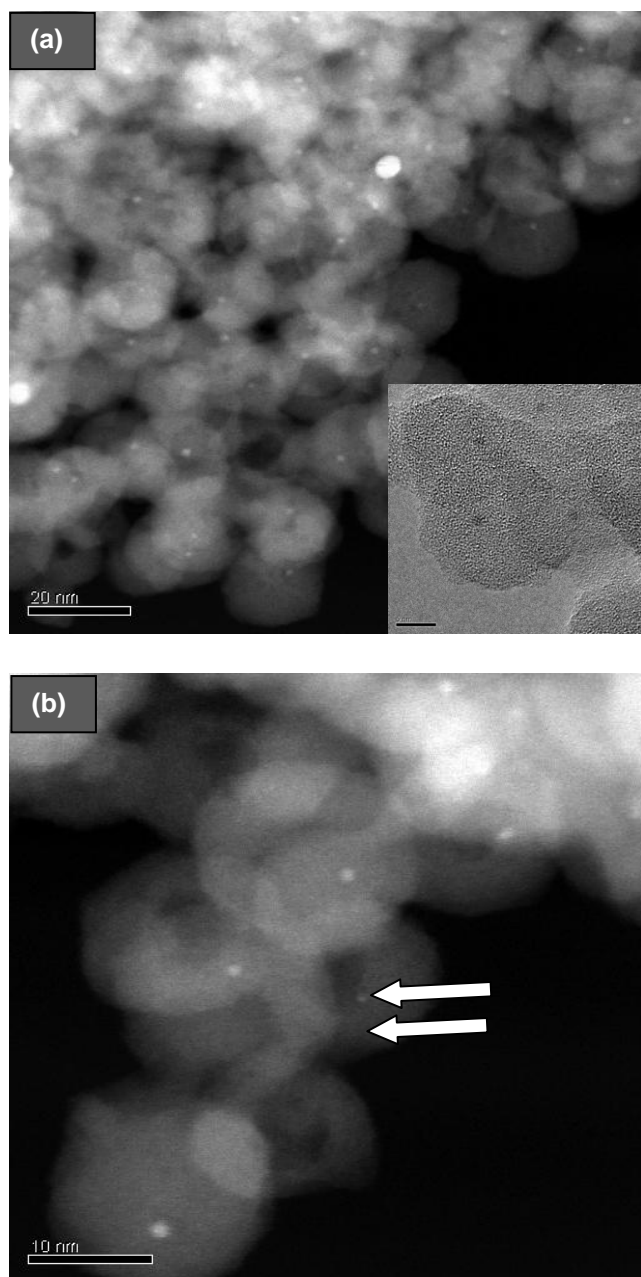


Fig. S18. Representative HAADF-STEM images (a,b) of Au@SiO₂-AP-C after catalytic reaction (inset showing TEM image).

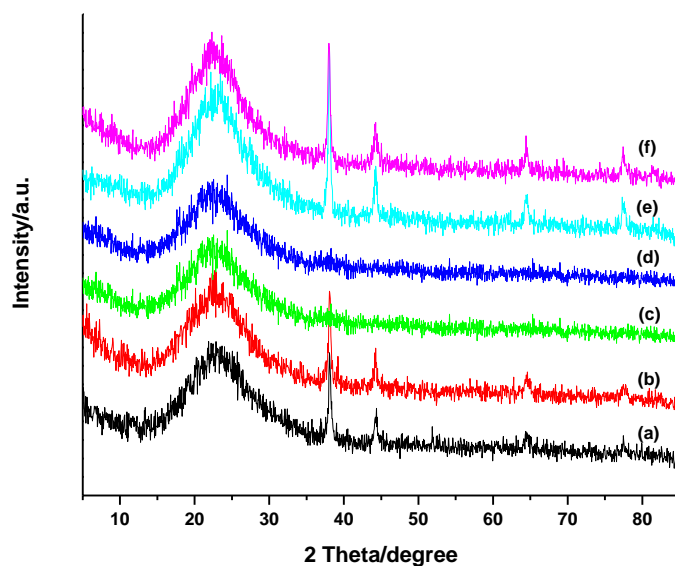


Fig. S19. Powder XRD profiles for Au@SiO₂ (a) before and (b) after catalysis, Au@SiO₂_EN (c) before and (d) after catalysis, and Au@SiO₂_AP (e) before and (f) after catalysis.

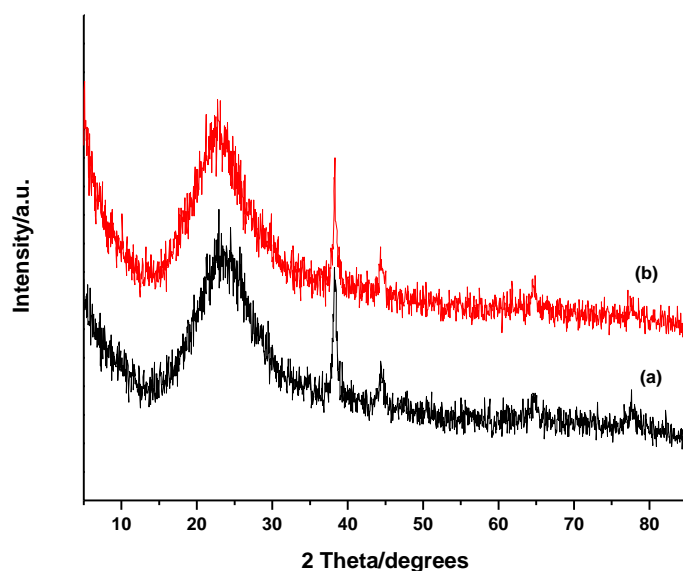


Fig. S20. Powder XRD profiles for Au@SiO₂_AP catalyst (prepared by using hydrazine as the reducing agent) (a) before and (b) after catalysis.

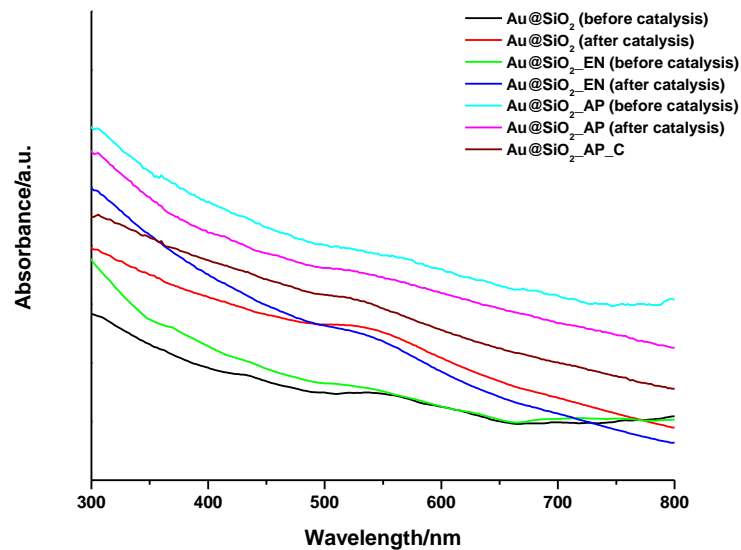


Fig. S21. UV-vis absorption spectra of Au@SiO₂, Au@SiO₂_EN, Au@SiO₂_AP, and Au@SiO₂_APW_C.

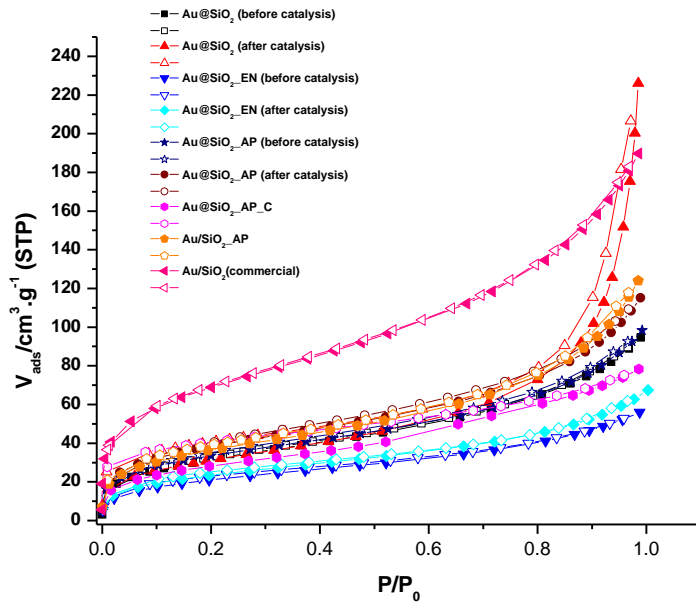


Fig. S22. Nitrogen adsorption isotherms of Au@SiO₂, Au@SiO₂_EN, Au@SiO₂_AP, Au@SiO₂_APW_C, Au/SiO₂_AP, and Au/SiO₂ (commercial) at 77 K.